

Supplementary Appendix

This appendix has been provided by the authors to give readers additional information about their work.

Supplement to: Bainbridge JWB, Mehat MS, Sundaram V, et al. Long-term effect of gene therapy on Leber's congenital amaurosis. *N Engl J Med* 2015;372:1887-97. DOI: [10.1056/NEJMoa1414221](https://doi.org/10.1056/NEJMoa1414221)

Supplementary Appendix

Table of Contents

| | |
|---|-----------|
| Supplementary Methods | 2 |
| Vector Manufacture and Delivery | 2 |
| Dark-adapted perimetry | 2 |
| Microperimetry | 3 |
| Vision-guided ambulatory mobility | 3 |
| Spectral sensitivity | 4 |
| AAV2 neutralising antibody assay | 5 |
| ELISA to detect circulating levels of IgA, IgG and IgM against AAV2 or rRPE65 | 5 |
| ELISpot | 6 |
| Optical coherence tomography..... | 7 |
| RPE65 expression levels in the human and dog eye | 7 |
| Vector administration in the dog model | 7 |
| Dog electroretinography | 8 |
| Dog vision testing..... | 8 |
| Dog retinal immunohistochemistry | 8 |
| Dog retinoid analysis..... | 9 |
| Supplementary Results | 10 |
| Figure S1. Retinal sensitivity by microperimetry..... | 10 |
| Figure S2. Topography of retinal sensitivity by microperimetry | 11 |
| Figure S3. Retinal sensitivity during extended dark adaptation..... | 12 |
| Figure S4. Spectral sensitivities | 13 |
| Figure S5. Visual acuity..... | 15 |
| Figure S6. Fundus photographs demonstrating intraocular inflammation. | 16 |
| Table S1. Summary of Adverse Events | 17 |
| Tables S2a –S2d. Immune Responses | 18 |
| Figure S7. Macular Thickness | 23 |
| References | 25 |

Supplementary Methods

Vector Manufacture and Delivery

The vector contains the human *RPE65* coding sequence driven by a 1400-bp fragment of the human *RPE65* promoter and terminated by the bovine growth hormone polyadenylation site as described elsewhere¹. Targeted Genetics Corporation produced the vector according to Good Manufacturing Practice guidelines with the use of a B50 packaging cell line, an adenovirus–adeno-associated virus hybrid shuttle vector containing the tgAAG76 vector genome, and an adenovirus-5 helper virus. The vector was filled in a buffered saline solution at a titer of 1×10^{11} vector genomes per mL and frozen in 1-mL aliquots at -70°C . Administration to participants was preceded by 20-gauge 3-port, pars-plana vitrectomy. Up to 1 mL of recombinant AAV2/2.*hRPE65p.hRPE65* was injected into the subretinal space using a 41-gauge cannula (de Juan, Synergetics). The injection of vector suspension was preceded by injection of a small volume (0.1 mL) of Ringer’s solution to establish a bleb, facilitating targeted delivery of vector suspension to the subretinal space. Involvement of the fovea was intended in all participants, where necessary by means of a fluid-air exchange to extend the induced retinal bleb to involve the central macula. To reduce the possibility of intraocular inflammation, participants were given a 5-week course of oral prednisolone, at a daily dose of 0.5 mg per kilogram of body weight for 1 week before administration of the vector, 1 mg per kilogram for the first week after administration, 0.5 mg per kilogram for the second week, 0.25 mg per kilogram for the third week, and 0.125 mg per kilogram for the fourth week. Participants received betamethasone and cefuroxime subconjunctivally at the completion of surgery and topical chloramphenicol 0.5 % four times a day for 7 days, dexamethasone 0.1 % four times a day for 4 weeks, and 1% atropine twice a day for 7 days after surgery.

Dark-adapted perimetry

In dark-adapted conditions using a short wavelength stimulus, sensitivities were measured at 76 locations in the central visual field using a modified Humphrey perimeter. Measurements were made between 60 and 240 minutes of dark adaptation using Goldman V stimuli of 200 ms duration. All testing followed a detailed standardized protocol, with controlled room lighting, dark-adaptation period and a fixed sequence of test patterns. The test is fully automated so there is little opportunity for experimenter bias. The participant’s eye position was continually monitored using an infrared camera. Reliability parameters were determined for each test including fixation losses, false negative and false positive responses according to the manufacturer's criteria. The change in sensitivity at each location

from baseline to 36 months' follow-up was evaluated with pointwise linear regression using PROGRESSOR[®] software². The number of loci that had a significant positive slope ($P < 0.05$) was plotted against time following intervention.

Microperimetry

Microperimetry was performed with a Nidek MP1 microperimeter (NAVIS software version 1.7.1, Nidek Technologies, Padova, Italy), using Goldman V stimuli of 200 ms duration. Following 10 minutes of dark adaptation a white fixation cross (31.8 cd/m^2) was displayed on a dim background (1.27 cd/m^2). All participants were tested with a central grid (68 points, $\pm 10^\circ$ from fixation) and a peripheral grid (55 points, $\pm 20^\circ$ horizontal and $4\text{-}20^\circ$ above fixation) using 4-2 adaptive staircase thresholding strategy. The Nidek MP1 microperimeter monitors the participant's eye position with an infrared camera and moves the stimulus to compensate for shifts in the direction of gaze. Reliability parameters were determined for each test including fixation losses, false negative and false positive responses. False positives were identified as positive responses to light projected onto a known blind spot (the optic nerve head); responses to the light indicate poor reliability. Microperimetry data were analyzed using a volumetric approach, Visual Field Modeling and Analysis (VFMA)³. VFMA can be applied to any static field data where the test locations and associated sensitivity data in dB can be exported. A thin-plate spline is fit through the sensitivity data points and the volume in dB-steradian (dB-sr) is determined by integration of the sensitivity of the visual field with the solid angle beneath the envelope. If the sensitivity at all points were at the maximum of 20 dB, the field volume would equal 5.67 dB-sr. Test-retest variability was determined with the one-way ANOVA method using multiple baseline measurements⁴.

Vision-guided ambulatory mobility

At baseline and 6 months after intervention, we measured vision-guided ambulatory navigation at the UCL Pedestrian Accessibility and Movement Environment Laboratory (PAMELA). PAMELA is a simulated outdoor sidewalk environment consisting of an 80 m^2 raised platform with concrete paving stones and street lamps. The platform was configured as 3 mobility tasks: 10 m straight walk through an open doorway; 13 m serpentine course through a simple maze with 8 barriers; and 10 m straight walk along a path with simulated curbstones. Illumination levels ranged from 240 lux (indoor office light) to 4 lux (night-time residential street lighting), with a 2 lux condition added for Participants 5 through 12. Testing was performed monocularly in counter-balanced order. Barriers in the maze were randomly positioned for each trial. Only the data from the maze were analysed for this

report and are presented as the number of errors made, which provides a more reliable assessment of visual ability during mobility testing than the time taken for course completion.⁵

Spectral sensitivity

The spectral sensitivity measurements were made using one channel of a standard, Maxwellian-view optical system illuminated by a 75-W Xe arc lamp. Details of the apparatus have been previously described⁶. Participants 5 through 8, 11 and 12 were measured using a bite-bar to maintain head position. For the youngest participants, 9 and 10, the system was reconfigured with a diffuser screen, so that the flickering stimuli could be freely viewed using just a chin-rest to restrict head movements. The target was a disc, 3.5° in visual diameter. There was no background light. To aid fixation, participants 5 through 8, 11 and 12 were instructed to fixate on a red spot produced by a small red LED presented 10° above the target. Thus sensitivity was measured at 10° in the superior retina. Participants 9 and 10 were simply asked to look slightly above the target. Participant 6 adjusted his fixation by about 6° nasal 4 months after gene therapy because when fixating there the stimulus “lit up”. Wavelengths were selected using a monochromator with a half-maximum bandwidth of 4 nm (Jobin Yvon, H-10) when the bite-bar was used or, because more light was needed with the diffuser, interference filters with half-maximum bandwidths of 10 nm (Ealing, Melles Griot) when the chin-rest and diffuser were used. Measurements were made at 450, 500, 550 and 600 nm when the monochromator was used and 469, 500, 550 and 600 nm when interference filters were used. Only data for 500 and 600 nm are presented here. The radiance of the beam was controlled by the fixed (Oriel) or variable neutral density filters, calibrated *in situ* (Rolyn Optics). Sinusoidal flicker was produced by pulse-width modulation of fast, liquid crystal light shutters (Displaytech). All participants dark-adapted for 40 minutes before the measurements. They interacted with the computer that controls the apparatus by means of keypad (or in the case of the younger participants, 7 through 11, by verbally instructing the experimenter who controlled the keypad), and received information and instructions via tones and a computer-controlled voice synthesizer. The method of adjustment was used to measure the visual responses at each wavelength. The observers adjusted the radiance of the target until they were satisfied that the flicker was just visible. Two buttons on the keypad increased or decreased the intensity of the target by 0.02 log₁₀ unit, two other buttons produced larger (0.10 log₁₀ unit) changes, and a fifth was pressed to indicate that the flicker was at threshold (i.e., just visible). Spectral sensitivity measurements were made in Participants 5 through 12 at baseline, and following vector administration at

approximately 2-month intervals for 12 months, and subsequently at 12-month intervals. Measurement of spectral sensitivity was introduced in the trial only after Participants 1 through 4 had received vector; for these we compared the responses of the study eye with those of the contralateral uninjected eye. Repeated measurements were used to calculate the mean spectral sensitivity and S.E.M. for each participant at each time-point.

In addition to dark-adapted settings, measurements were made in the 3 oldest participants administered the higher dose, during the cone plateau following an intense bleach. The bleaching light was a white Ganzfeld (full-field) of 5.50 log₁₀ scotopic trolands viewed for 30 s. This light bleaches more than 60% of the rod photopigment in normal observers⁷ and leads to a cone plateau that lasts between 3 and 10 minutes following the bleach. Since bleaching can be uncomfortable (and since we found no evidence for dark-adapted rod function in the younger participants), we performed these measurements only in the 3 oldest participants administered the higher dose (Participants 5, 6 and 12).

AAV2 neutralising antibody assay

2.5x10³ HEK-293T cells in 50µL complete media (DMEM, 10% FBS, Penicillin, Streptomycin) were seeded per well into in a 96-well plate (Nunc™ Delta Surface). At least four hours after seeding, AAV2-CMV-GFP was incubated at 37°C for an hour with a range of 1:2 serial dilutions of test serum from the participant, prior to (baseline) and at defined time-points following administration of the clinical grade AAV2/2-*hrPE65p-RPE65* vector. Each dilution of participant sera mixed with AAV2-CMV-GFP was performed in triplicate and the incubated mixtures were added to the cultured HEK-293T cells. 48 hours later, the infectivity of the AAV2-CMV-GFP was investigated by counting the number of GFP positive cells in each well. The presence of neutralising antibodies within the serum samples was then calculated. The titre of neutralising antibodies was expressed as the dilution of serum that yields 50% of the number of GFP positive cells relative to wells where no serum was incubated with vector (positive control). The assay was performed according to written previously established protocols and quality controls were included in each assay run to guarantee optimal quality of the data generated.

ELISA to detect circulating levels of IgA, IgG and IgM against AAV2 or rRPE65

Immunosorb ELISA plates were coated overnight at 4°C with either 2x10⁹ vector genome per mL clinical grade AAV2/2-*hrPE65p.hrPE65* or recombinant human RPE65 (hrPE65) protein (kind gift from The University of Canterbury) in carbonate buffer (150mM Na₂CO₃, 350mM NaHCO₃, pH 9.6). The wells were washed with 0.05% Tween PBS and blocked for 1 hour at

37°C with 5% sucrose (w/v), 1% BSA (w/v), 0.05% Tween 20 (v/v) in PBS. After washing the blocked wells with 0.05% Tween PBS, the participants' sera were diluted 1:100 and 1:200 in 1% (w/v) skimmed milk powder in PBS. Diluted sera were added to the coated wells and incubated at room temperature for 2 hours. Any serum immunoglobulins specific for AAV2 or hRPE65 will bind to AAV2 surface antigens or hRPE65, respectively. As a positive control, mouse anti-AAV2 antibody A20 (Fitzgerald), diluted 1:200, was used to detect the AAV2/2.hRPE65p.hRPE65. Serum anti-AAV2 or hRPE65 immunoglobulins were detected by a goat anti-human IgG, A, M - horseradish peroxidase (HRP)-labelled F(ab')₂ diluted 1:2000 (AbD Serotec STAR 90P). For the positive control mouse anti-AAV2 antibody wells, a goat anti-mouse IgG-peroxidase conjugated antibody (Thermo Scientific) was used at a 1:5000 dilution. HRP activity was visualized by a TMB colour reaction, stopping the reaction with 1M HCl. Optical density values obtained with test sera following administration of AAV2/2.hRPE65p.hRPE65 vector were compared to baseline values and the amount of binding of Ig to the antigen within test serum was expressed as a percentage of the baseline.

ELISpot

Peripheral Blood Mononuclear Cells (PBMCs) were isolated from fresh venous blood containing EDTA as an anti-coagulant. The blood was diluted 1:1 in PBS. In a 50mL Falcon tube containing Lymphoprep (10 mL per 15 mL of diluted blood) the blood was layered on top of the Lymphoprep (Axis-Shield) and centrifuged at 2200 rpm at 22°C for 22 minutes. The PBMCs present at the interface between the Lymphoprep and serum were aspirated and washed in 50ml PBS and subsequently centrifuged at 1500 rpm for 10 mins. The wash was repeated to dilute out any Lymphoprep. The PBMCs were re-suspended into 3-5 mL complete CTL-Test media (CTL Europe) containing 1% (v/v) L-glutamine + 1% (v/v) antibiotic/antimycotic (Invitrogen). Wells of an immobilon P plate (Millipore) were coated for 2 hours at 37°C with 10 µg/mL capture antibody specific for IFN γ (Mabtech, 1-D1K). After washing the wells with PBS, the wells were blocked with 50 µL foetal calf serum at 37°C for 1 hour. After washing the wells with PBS, 100 µL PBMCs were added to each well at an adjusted concentration of 2.5x10⁶ cells/mL and then incubated at 37°C for 48 hours in the presence of clinical grade AAV2/2.hRPE65p.hRPE65 vector particles (100 µL 1x10⁸ vg/mL were added per well). T-cells that responded to the AAV2/2.hRPE65p.hRPE65 vector secreted the pro-inflammatory cytokine IFN γ . Negative control wells contained PBMCs cultured in media only. Positive control wells contained 100 µL CTL-Test media containing 100ng/mL anti-CD3 antibody, which activated all T-cells in a non-specific manner. 48 hours afterwards, a biotinylated antibody specific to IFN γ (Mabtech, 7-B6-1) was added at a final

concentration of 1 µg/mL, for 2 hours at room temperature. After washing the wells, 100 µL avidin-alkaline phosphatase (AP) conjugate, ExtrAvidin (Sigma) diluted 1:1000 in PBS was added. Upon addition of AP substrate (BioRad) spots of color were observed where reactive T cells were positioned. These were counted using an ELISpot plate reader. Test values were considered positive when the mean number of spots was more than twice the mean number of spots on the negative control samples.

Optical coherence tomography

We performed OCT scanning in Participants 1 through 4 using time-domain scanning only; in Participants 5 through 12 we also used Spectral-Domain OCT (SD-OCT) (Spectralis, Heidelberg Engineering, Germany) including line-scans or volume-scans at the horizontal meridian. The volume acquisition protocol involved 49-B scans (124 micron space between scans) covering an area of 20° by 20°. Foveal thickness was determined using the automated retinal thickness measurements between the inner limiting membrane (ILM) and the inner border of the line of back-reflection indicating the RPE; this was checked for segmentation errors. The integrity of the external limiting membrane (ELM) and inner segment (IS)/outer segment (OS) junction or inner segment ellipsoid (ISe) was evaluated. The re-test variability used for time-domain and SD-OCT was 18 and 15 microns, respectively⁹. These assessments were performed at 2-monthly intervals during the first 12 months, and then annually for 3 years following vector administration.

RPE65 expression levels in the human and dog eye

Total RNA was isolated from full-thickness retina of 4 human and 4 wild type dog samples using the Qiagen RNeasy Mini kit according to the manufacturer's protocol. Absolute *RPE65* mRNA levels were measured by real-time PCR against DNA standards using SYBR-Gold quantification and species dependent primers. Absolute quantification of *ACTB* mRNA levels was used for loading correction of *RPE65* mRNA levels. Expression of RPE65 in human and canine retina was compared using a 2-tailed t-test.

Vector administration in the dog model

Animals came from a colony maintained at the Michigan State University Comparative Ophthalmology Laboratory and were cared for in compliance with the Association for Research in Vision and Ophthalmology statement for the Use of Animals in Ophthalmic and Vision Research with the approval of the Institutional Committee. To explore the relationship between vector dose, ERG activity and vision, we administered

rAAV2/2.*hrPE65p.hrPE65* into the eyes of 12 young Rpe65-deficient dogs as previously described¹⁰. In each instance a volume of 250 μ L of vector was injected giving a total number of viral particles injected of: 8×10^8 vg (Group 4, n=3), 4×10^9 vg (Group 3, n=3), 2×10^{10} vg (Group 2, n=3) and 1×10^{11} vg (Group 1, n=3).

Dog electroretinography

Electroretinography in dogs was performed as previously described¹⁰. To assess rod responses the dark-adapted b-wave amplitude in response to a flash of 1 cdS/m^2 were used. The amplitudes at this flash intensity are below a criterion threshold response of 5 μ V in untreated *Rpe65*^{-/-} dogs. ERG data of treated animals were compared with untreated control animals using ANOVA with Dunnett's multiple comparison test.

Dog vision testing

We measured vision in dogs at baseline and 2 months following vector administration using a 4-choice device¹¹ and used linear regression analysis to determine its relationship with vector dose. To determine whether there was an improvement in vision without a concomitant improvement in ERG, we compared visual behavior in the group of animals treated with the highest vector dose that unambiguously failed to improve the ERG with that of the untreated animals using an unpaired 2-tailed t-test.

Dog retinal immunohistochemistry

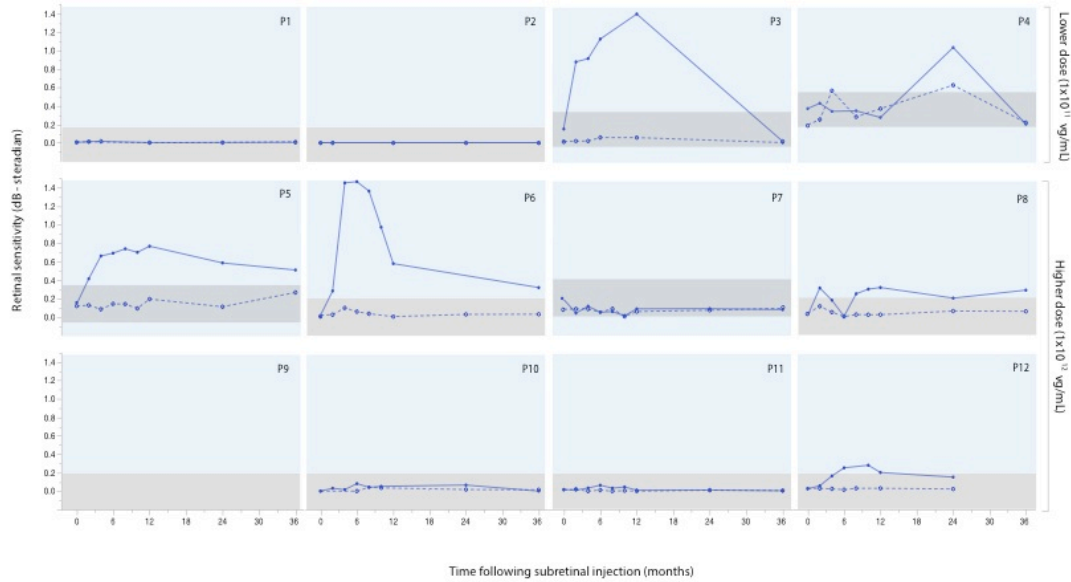
Dogs were dark adapted for 1 hour prior to euthanasia. Euthanasia and all subsequent tissue dissection were performed with the aid of dim red illumination. Eyes were enucleated and placed on ice prior to dissection. 3 mm retinal, choroidal and scleral punch biopsies were obtained from 4 quadrants within the retina (superior nasal, superior temporal, inferior nasal and inferior temporal) and fixed for 2 h in 2 % paraformaldehyde. Biopsies were embedded in OCT and 14 μ m sections were used for immunohistochemistry. The remaining retina was divided into 4 quadrants using horizontal and vertical cuts. The retina was manually separated from the choroid/RPE and retinal and choroid/RPE quadrants were frozen separately on dry ice. Quadrants were kept in the dark at $-80 \text{ }^\circ\text{C}$ until retinoid processing. Immunohistochemistry for RPE65 protein was performed as previously described¹² utilizing a secondary antibody conjugated to AlexaFluor 594. Confocal images (Olympus Fluoview 1000) were obtained to examine the IHC signal and for comparison, the autofluorescence signal.

Dog retinoid analysis

Dogs were dark-adapted for 1 hour, then were euthanized, and eyes enucleated. In the dark, and on ice, anterior segments and retinas were removed and the RPE/choroid was dissected into four quadrants (Superior Temporal (ST), Superior Nasal (SN), Inferior Temporal (IT), and Inferior Nasal (IN)). Quadrants were collected and frozen at -80°C. Retinoids were extracted using a modification of a previously described method¹³. Briefly, under dim red light and on ice, each quadrant was homogenized then sonicated in 2 mL chloroform:methanol:hydroxylamine (2 M) (3:6:1) and incubated at room temperature for 2 min. Next, 200 µL chloroform and 240 µL water were added, and each sample was vortexed and centrifuged at 14,000 rpm for 5 min. The lower phase was collected, the solvent was evaporated under nitrogen, and the sample was dissolved in hexane. Retinoids in the extracts were identified and quantified by high-performance liquid chromatography (HPLC) analysis, using a Waters Alliance separation module and photodiode array detector with a Supelcosil LC-31 column (25 cm by 4.6 mm by 3 µm) developed with 5% 1,4-dioxane in hexane¹⁴.

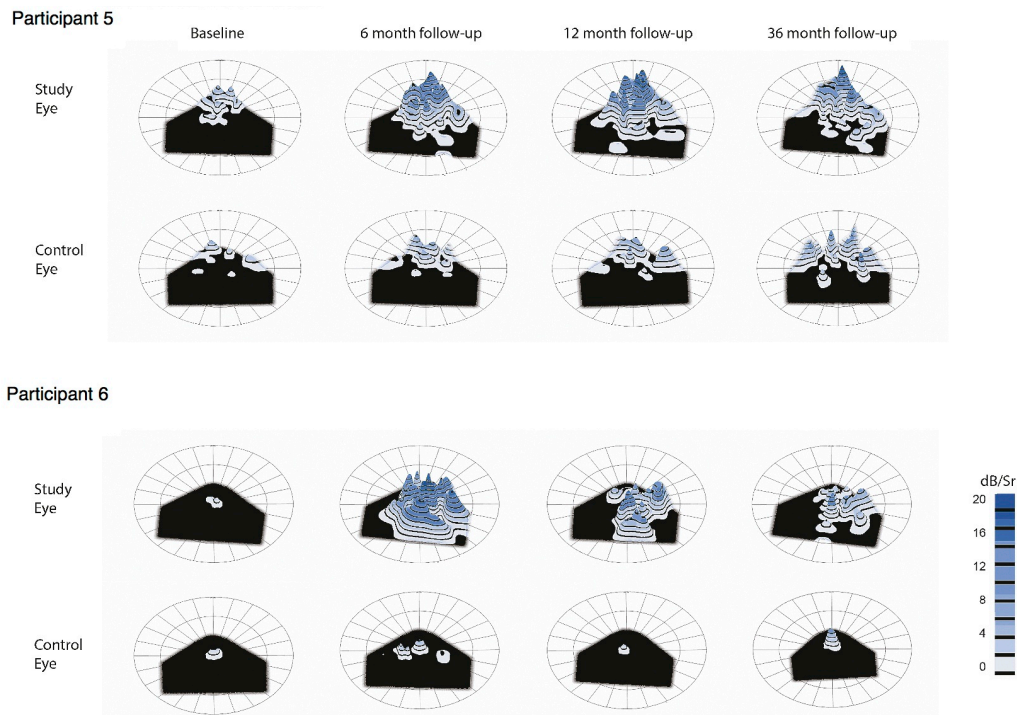
Supplementary Results

Figure S1. Retinal sensitivity by microperimetry



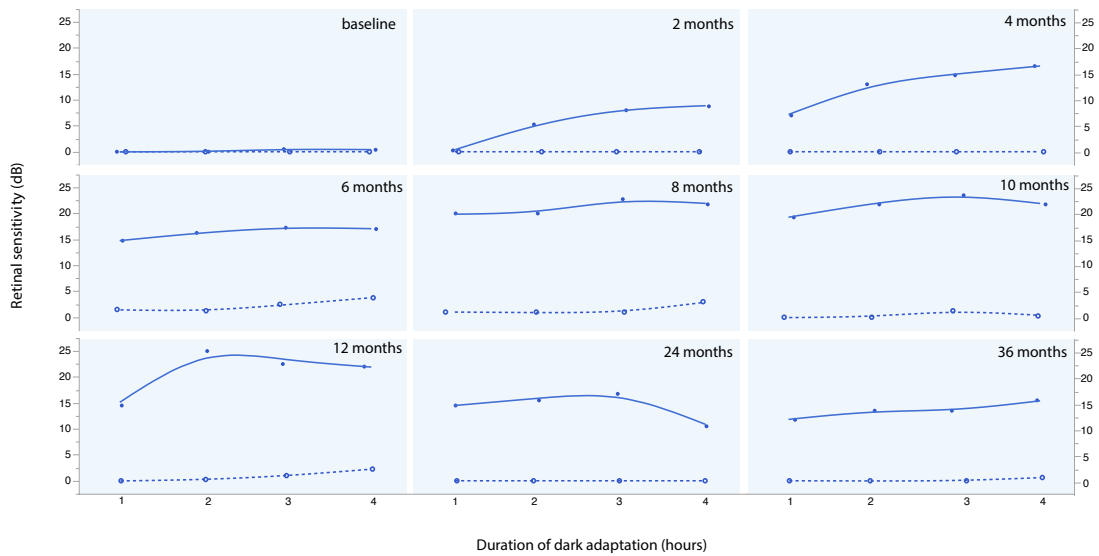
Volumetric retinal sensitivity in dB-sr is plotted over 3 years for each participant. Data from study eyes are plotted with filled symbols connected by a solid line; data from the contralateral untreated control eyes are plotted with open symbols connected by dashed lines. Test-retest variability for each participant was determined with the one-way ANOVA method using multiple baseline measurements⁴ and is indicated by the grey areas on each plot. Participants 3 (P3), 5, and 6 show clear improvement of retinal sensitivity by around month 6 followed by a decline in sensitivity, returning to near baseline levels by 3 years. Participants 8 and 12 also show some improvement. Apparent improvement in participant 4 at 24 months is not considered reliable because of a similar change apparent in his untreated eye. Participant 9 was unable to comply with the testing protocol.

Figure S2. Topography of retinal sensitivity by microperimetry



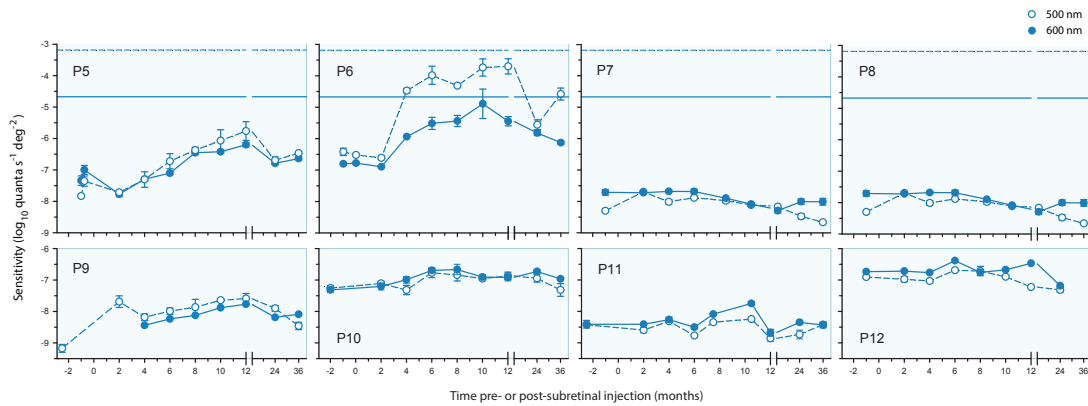
For Participants 5 and 6, 3-dimensional topographical maps were constructed by interpolation of sensitivities at the test loci. Data from the central and peripheral fields were combined and the resulting hill of vision was quantified with Visual Field Modeling and Analysis (VFMA) software developed by one of the authors³. Black regions indicate no measurable retinal sensitivity. Participant 5 shows an increase in the volume of the hill of vision for the treated eye at 6 months and 12 months followed by a slight decrease in sensitivity at 36 months. Participant 6 shows a more dramatic increase in sensitivity at 6 months (up to 4.8 log₁₀ units) followed by a steeper decline in sensitivity out to 36 months.

Figure S3. Retinal sensitivity during extended dark adaptation



For Participant 6 the mean sensitivity during 4 hours of dark adaptation in both their study eye (continuous line) and contralateral control eye (broken line) at intervals during the 3-year duration of the trial is presented. Dark adaptation normally reaches peak retinal sensitivity within 1 hour. Following vector administration for RPE65 deficiency, dark adaptation is improved, but at 2 months and 4 months the time to reach maximum sensitivity remains abnormally prolonged.

Figure S4. Spectral sensitivities



Dark-adapted sensitivities in $\log \text{ quanta s}^{-1} \text{ deg}^{-2}$ for detecting 1-Hz 500-nm flicker (open circles) and 600-nm flicker (filled circles) plotted as a function of the number of months before and after gene therapy treatment. Data for the 8 participants (Participants 5 through 12) administered the higher dose are shown in separate panels. The error bars show ± 1 standard error for each of the 500-nm (open circles with dashed lines) and 600-nm (closed circles with solid lines) dark-adapted threshold measurements. With some exceptions, the standard errors for each participant are roughly constant over the course of the experiment. Sensitivity measurements that consistently deviate by more than 2 standard errors from earlier measurements are considered to be significantly different. The ordinates are to scale. For comparison, in the top four panels, for participants 5 through 8, the mean dark-adapted sensitivities for 9 normal participants for detecting 1-Hz 500-nm and 600-nm flicker are plotted as the dashed and solid blue horizontal lines, respectively.

For Participant 6, the flicker sensitivities approached those of the mean normal observer at 500 and 600 nm. Before vector administration, and up to 2 months later, the dark-adapted spectral sensitivities are consistent with 1-Hz flicker detection by middle and/or long-wavelength sensitive cones. After vector administration the dark-adapted sensitivities are substantially improved at both 500 and 600 nm, and the proportionately greater improvement (by approximately 1.5 log unit) at 500 nm than at 600 nm indicates recovery of rod function. Further proof that the dark-adapted spectral sensitivities after treatment are mediated by rods can be obtained by measuring spectral sensitivity between 3 and 12 minutes during the cone plateau after an intense bleach when cones but not rods have recovered (Figure S4b), during which the “rod-bleach” spectral sensitivities are substantially lower and consistent with flicker detection being mediated by cones.

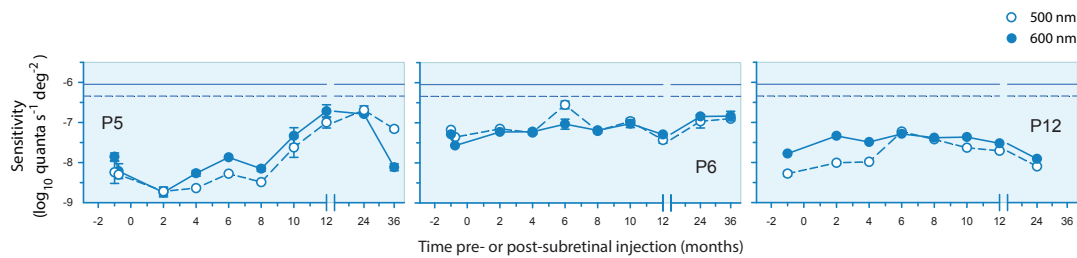
For Participant 5, like 6, there is a sensitivity improvement after intervention, starting to increase 2 months after the treatment and gradually rising by nearly 2 \log_{10} units at 500 nm

and by about 1.5 \log_{10} unit at 600 nm until 12 months following intervention, after which they decline slightly. The dark-adapted spectral sensitivities for Participant 5 after vector administration are consistent with detection by rods at 500 nm, and by both rods and L/M cones at 600 nm.

The dark-adapted spectral sensitivities for the other 6 participants administered the higher dose vector showed relatively little change in sensitivity. In general, their spectral sensitivities for detecting 1-Hz flicker remained cone-like before and after treatment, consistent with detection by L/M cones. Reliable data at 600 nm could not be obtained from Participant 9 until four months after vector administration.

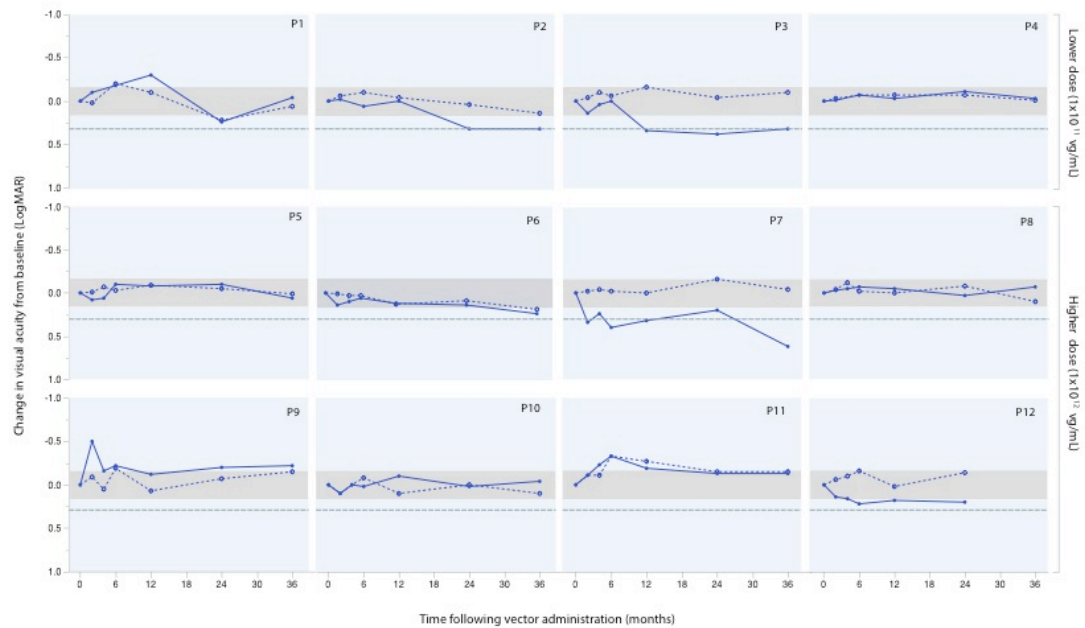
In one participant (Participant 3), who received the lower dose vector, spectral sensitivities (measured following intervention only) were substantially greater (in excess of 1 log-fold) in the study eye than the control eye at a wavelength suggesting improved rod function (data not shown).

Figure S4b. Cone-plateau spectral sensitivities at 500 and 600 nm



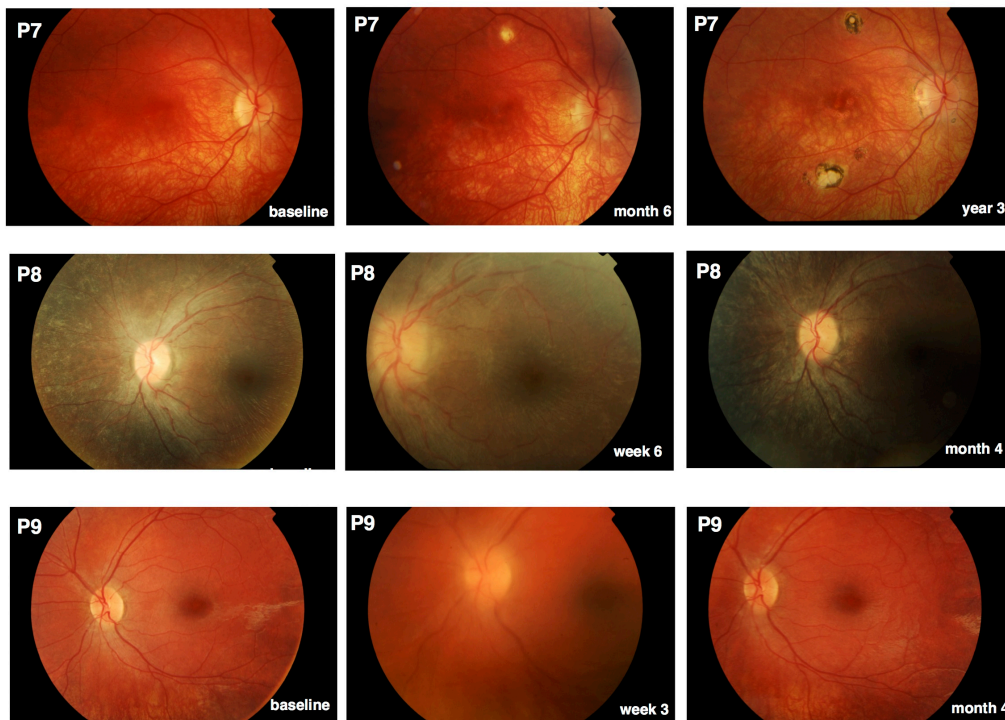
Cone plateau measurements, which were made only in the older participants (Participants 5, 6 and 12) because the bleach was relatively uncomfortable, are consistent with cone detection. Each panel shows the cone-plateau sensitivities in \log quanta s^{-1} deg^{-2} for detecting 1-Hz 500-nm flicker (open circles with dashed lines) and 600-nm flicker (filled circles with solid lines) plotted as a function of the number of months before and after gene therapy treatment. Data for the 3 adult participants (Participants 5, 6 and 12) administered the higher dose are shown in separate panels. Error bars ± 1 S.E.M. For comparison, the mean cone-plateau sensitivities for 9 normal participants for detecting 1-Hz 500-nm and 600-nm flicker are plotted in each panel as the dashed and solid horizontal lines, respectively. Not unexpectedly, the cone-plateau data are consistent with cone detection. The data for Participants 6 and 12 show relatively little change after intervention. However, the data for Participant 5 show evidence of an improvement in cone function following vector administration.

Figure S5. Visual acuity



For each of the 12 participants, a continuous line indicates the visual acuity of the study eye, and a dotted line indicates that of the contralateral control eye. Baseline visual acuity is presented as the mean of 3 separate measurements. The grey areas indicate test-retest variability, determined using the multiple baseline measurements with the one-way ANOVA method.⁴ A line at 0.3 LogMAR indicates the change in acuity equating to the conventional criteria for clinical significance. For Participant 11, an apparent improvement in visual acuity in the study eye was accompanied by a similar improvement in the contralateral eye. A clinically significant decline in visual acuity was measured in 2 participants (Participants 3 and 7), and a more modest but sustained decline in visual acuity was apparent in Participant 12. Participants 7 and 12 described some subjective deterioration of vision.

Figure S6. Fundus photographs demonstrating intraocular inflammation.



Participant 7 developed mild anterior uveitis 2 weeks following completion of the standard postoperative course of topical corticosteroids. The anterior uveitis resolved following a further 6-week course of topical corticosteroids but was followed by the gradual development of focal chorioretinal pigmentary changes (month 6, year 3). Two participants (8 and 9) developed asymptomatic episodes of posterior intraocular inflammation in their study eye. Participant 8 developed mild vitritis, optic disc swelling, and retinal vascular tortuosity and sheathing evident 6 weeks following vector administration. The inflammation improved substantially within 2 weeks of a further course of oral prednisolone and topical dexamethasone, which was subsequently tapered and discontinued after 2 months (month 4). Participant 9 developed similar signs, evident 3 weeks following vector administration. Clinical signs of inflammation resolved fully within 2 months of surgery following administration of an increased dose of postoperative oral prednisolone (month 4).

Table S1. Summary of Adverse Events

| Adverse Event | <i>Number of participants affected</i> | <i>Number of events</i> |
|------------------------------------|--|-------------------------|
| Any adverse event | | 38 |
| <i>1. Ocular</i> | | |
| 1.1 Any | 1 | 1 |
| 1.2 Anterior uveitis | 1 | 1 |
| 1.3 Posterior uveitis | 2 | 2 |
| 1.4 Increased intraocular pressure | 3 | 3 |
| 1.5 Conjunctivitis | 2 | 2 |
| 1.6 Eye discharge | 1 | 1 |
| <i>2. Respiratory</i> | | |
| 2.1 Any | 0 | 0 |
| 2.2 Cough | 1 | 1 |
| <i>3. Skin</i> | | |
| 3.1 Any | 0 | 0 |
| 3.2 Cellulitis | 1 | 1 |
| 3.3 Acne | 1 | 1 |
| <i>4. Allergy</i> | | |
| 4.1 Any | 1 | 1 |
| <i>5. Neurological</i> | | |
| 5.1 Any | 1 | 1 |
| 5.2 Change in mood | 4 | 4 |
| 5.3 Sleep disturbance | 1 | 1 |
| <i>6. Pain</i> | | |
| 6.1 Any | 1 | 1 |
| 6.2 Eye pain | 5 | 5 |
| <i>7. Gastrointestinal</i> | | |
| 7.1 Any | 0 | 0 |
| 7.2 Change in body weight | 1 | 1 |
| 7.3 Change in appetite | 1 | 1 |
| 7.4 Reflux | 1 | 1 |
| 7.5 Nausea and vomiting | 2 | 2 |
| <i>8. Genitourinary</i> | | |
| 8.1 Any | 0 | 0 |
| 8.2 Proteinuria | 1 | 1 |
| 8.3 Glycosuria | 2 | 2 |
| <i>9. Constitutional</i> | | |
| 9.1 Any | 1 | 1 |
| 9.2 Fatigue | 1 | 1 |
| <i>10. Serious adverse event</i> | 2 | 2 |

Tables S2a –S2d. Immune Responses

Table S2a. Circulating neutralizing antibodies against AAV2

| Participant | Baseline | Day 1 | Wk2 | Wk4 | Mnth4 | Yr 1 | Yr3 |
|-------------|----------|-------|------|------|-------|------|-----|
| 1 | 4 | 3 | 4 | 6 | 6 | 4 | 16 |
| 2 | neat | neat | neat | 2 | neat | 3 | 3 |
| 3 | neat | neat | neat | neat | neat | neat | 2 |
| 4 | 512 | 512 | 512 | 1024 | 1024 | 512 | 200 |
| 5 | 4 | 4 | neat | neat | neat | 2 | 1.5 |
| 6 | 2 | neat | 1.5 | neat | neat | neat | 1.5 |
| 7 | 2 | 1.5 | neat | 256 | 1024 | 700 | 512 |
| 8 | 1.5 | neat | 1.5 | neat | 16 | 6 | 2 |
| 9 | 4 | ... | ... | 125 | 32 | ... | 64 |
| 10 | 1.5 | neat | neat | 2 | 3 | neat | 16 |
| 11 | neat | 1.5 | 1.5 | neat | neat | 5 | 2 |
| 12 | neat | neat | 1.5 | 1.5 | 3 | 2 | 2 |

An AAV2 vector encoding green fluorescent protein, AAV2-CMV-GFP, was incubated with a range of 1:2 serial dilutions of test serum from the patient, prior to (baseline) and following administration of the AAV2/2.*hrPE65p.hrPE65* vector. The incubated AAV2-CMV-GFP and patient sera were added to cultured 293T cells. 48 hours later, the infectivity of the AAV2-CMV-GFP was investigated by counting the number of GFP positive cells in each well. The presence of neutralizing antibodies within the serum samples was then calculated. The titre of neutralizing antibodies is expressed as the dilution of serum that yields 50% of the number of GFP positive cells relative to wells where no serum was incubated with vector.

Table S2b. Serum ELISA to detect circulating levels of IgA, IgG and IgM against rRPE65

| Participant | Day 1 | Wk2 | Wk4 | Mnth4 | Yr 1 | Yr3 |
|-------------|-------|-------|-------|-------|-------|-------|
| 1 | 116 | 70.3 | 97.1 | 101.1 | 134.5 | 160 |
| 2 | 84 | 102.2 | 124.7 | 89.6 | 65.2 | 98.4 |
| 3 | 99.3 | 90.3 | 81.5 | 94.5 | 130.6 | 130.7 |
| 4 | 100.4 | 100 | 86.2 | 88.4 | 84.9 | 148.3 |
| 5 | 111.9 | 135.5 | 169.1 | 93.6 | 96.5 | 127 |
| 6 | 123.9 | 89.6 | 92.9 | 99.7 | 87.2 | 109 |
| 7 | 91 | 96 | 103 | 86 | 100 | ... |
| 8 | 104.3 | 125.3 | 43.6 | 59.2 | 53.5 | ... |
| 9 | ... | ... | 110.2 | 96 | ... | ... |
| 10 | 131.3 | 98.4 | 116.7 | 114 | 102.7 | ... |
| 11 | 83.3 | 110.7 | 88.6 | 90.4 | 95.6 | ... |
| 12 | 91.8 | 93.3 | 96.6 | 96.8 | 106 | ... |

Participants' sera were added to wells coated with recombinant human RPE65. Any serum immunoglobulins (Ig) specific for RPE65 will bind to the recombinant protein. Serum anti-RPE65 Ig were detected by a goat anti-human IgG,A,M - horseradish peroxidase (HRP) - labelled antibody. HRP activity was visualized by a TMB color reaction and read as optical densities (OD). The OD values obtained with test sera following administration of AAV2/2.hRPE65p.hRPE65 vector were compared to baseline values. Binding of Ig to the antigen within test serum is expressed as a percentage of the baseline.

Table S2c. Serum ELISA to detect circulating levels of IgA, IgG and IgM against AAV2

| Participant | Day 1 | Wk2 | Wk4 | Mnth4 | Yr 1 | Yr3 |
|-------------|-------|-------|-------|-------|-------|-------|
| 1 | 112.5 | 88.4 | 103 | 50.5 | 106.3 | 108.1 |
| 2 | 74 | 110 | 86.2 | 89.6 | 70.3 | 74.4 |
| 3 | 95.7 | 59 | 78.2 | 95.2 | 143 | 82.9 |
| 4 | 82.7 | 93 | 70.5 | 88.7 | 79.6 | 130 |
| 5 | 85.3 | 112 | 222.6 | 143.5 | 53 | 179 |
| 6 | 100.4 | 112.2 | 117.5 | 123.4 | 125.8 | 95 |
| 7 | 121.4 | 117.5 | 182.5 | 261.9 | 139.2 | 322.8 |
| 8 | 87.2 | 98.6 | 123.9 | 100.5 | 72.9 | 34.2 |
| 9 | ... | ... | 99.9 | 116 | ... | 31.2 |
| 10 | 109.6 | 91.6 | 95.6 | 95.2 | 97.3 | 47.2 |
| 11 | 95.7 | 107.6 | 101.7 | 98.7 | 95.6 | 39.4 |
| 12 | 113 | 98.4 | 97.4 | 113 | 100.9 | ... |

Participants' sera were added to wells coated with clinical grade AAV2/2.hRPE65p.hRPE65. Any serum immunoglobulins (Ig) specific for AAV2 will bind to AAV2 surface antigens. Serum anti-AAV2 Ig were detected by a goat anti-human IgG,A,M - horseradish peroxidase(HRP)-labelled antibody. HRP activity was visualized by a TMB color reaction and read as optical densities (OD). The OD values obtained with test sera following administration of AAV2/2.hRPE65p.hRPE65 vector were compared to baseline values and the amount of binding of Ig to the antigen within test serum is expressed as a percentage of the baseline.

Table S2d. ELISpot assay to detect secretion of the Th1 cytokine IFN γ

| Participant | Test | Base | Day 1 | Wk2 | Wk4 | Mnth4 | Yr 1 | Yr3 |
|-------------|----------|------|-------|------|------|-------|------|------|
| 1 | Negative | 7 | 14 | 8 | 13 | 89 | 74 | 305 |
| | Positive | >300 | >300 | >300 | >300 | >300 | 500 | 500 |
| | AAV | 25 | 25 | 9 | 21 | 75 | 119 | 271 |
| 2 | Negative | 3.5 | 0 | 4 | 4 | 1 | 20 | 3 |
| | Positive | >300 | 374 | >300 | >300 | >300 | 500 | 406 |
| | AAV | 5.3 | 1 | 3 | 4 | 3 | 24 | 3 |
| 3 | Negative | 11 | 13 | 6 | 7 | 89 | 14 | 20 |
| | Positive | >300 | >300 | >300 | >300 | >300 | 341 | >500 |
| | AAV | 15 | 21 | 13 | 9 | 116 | 0 | 26 |
| 4 | Negative | 143 | 155 | 6 | 4 | 7 | 6 | 26 |
| | Positive | >300 | >300 | >300 | >300 | 696 | 147 | 615 |
| | AAV | 155 | 118 | 4 | 7 | 11 | 9 | 7 |
| 5 | Negative | 3 | 2 | 4 | 6 | 42 | 14 | 2.5 |
| | Positive | 568 | 569 | 455 | >500 | 500 | 575 | 469 |
| | AAV | 1 | 4 | 4 | 10 | 21 | 6 | 6.3 |
| 6 | Negative | 2 | 0 | 8 | 7 | 3 | 8 | 7.5 |
| | Positive | 580 | >500 | 500 | 913 | 419 | 475 | 362 |
| | AAV | 3 | 2 | 5 | 5 | 1 | 4 | 8.7 |
| 7 | Negative | 10 | 3 | 6 | 34 | 13 | 17 | 2 |
| | Positive | 451 | 388 | 444 | 500 | 327 | 425 | 323 |
| | AAV | 12 | 5 | 8 | 70 | 13 | 12 | 1.66 |
| 8 | Negative | 12 | 1 | 8 | 5 | 5 | ... | 0.5 |
| | Positive | 400 | 459 | 555 | 471 | 399 | ... | 273 |
| | AAV | 12 | 6 | 11 | 1 | 3 | ... | 0.6 |
| 9 | Negative | 66 | ... | ... | 65 | ... | ... | 1.5 |
| | Positive | 471 | ... | ... | 576 | ... | ... | 432 |
| | AAV | 56 | ... | ... | 57 | ... | ... | 0.6 |
| 10 | Negative | 16 | 9 | 3 | 11 | 8 | 1 | 5 |
| | Positive | 654 | 573 | 550 | 562 | 494 | 482 | 555 |
| | AAV | 30 | 9 | 4 | 25 | 5 | 1 | 8.6 |
| 11 | Negative | 6 | 1 | 5 | 5 | 13 | 8 | 3 |
| | Positive | 447 | 461 | 464 | 410 | 613 | 370 | 370 |
| | AAV | 13 | 1 | 6 | 2 | 17 | 13.3 | 1 |
| 12 | Negative | 19 | 4 | 2 | 21 | 9 | 4 | ... |
| | Positive | 500 | 604 | 496 | 500 | 650 | 650 | ... |
| | AAV | 13 | 10 | 1 | 19 | 12 | 19 | ... |

Peripheral Blood Mononuclear Cells (PBMCs) isolated from fresh blood were added to wells coated with a capture antibody specific for IFN γ and then incubated for 48 hours in the presence of whole clinical grade AAV2/2.*hrPE65p.hrPE65* vector particles. T-cells that respond to the AAV2/2.*hrPE65p.hrPE65* vector secrete the pro-inflammatory cytokine IFN γ . Negative control wells contained PBMCs cultured in media only and positive control wells contained anti-CD3 antibody, which activates all T-cells in a non-specific manner. A biotinylated antibody was added specific to IFN γ and an avidin-alkaline phosphatase (AP) conjugate was added. Upon addition of AP, substrate spots of color were observed where reactive T cells were positioned, and were counted using an ELISpot plate reader.

Figure S7. Macular Thickness

Fig S7a: Macular thickness during the 3-year trial is presented for both the study eye (continuous line) and contralateral control eye (broken line) of each of the 12 participants. The grey areas indicate test-retest variability, determined using multiple baseline measurements with the one-way ANOVA method.⁴ The test-retest variability was significantly greater in Participants 1 through 4 because OCT imaging at baseline was performed in these using time-domain scanning; in Participants 5 through 12 the use of a spectral-domain device reduced the measurement variability substantially. Vector administration involved the fovea in all except Participants 9 and 11.

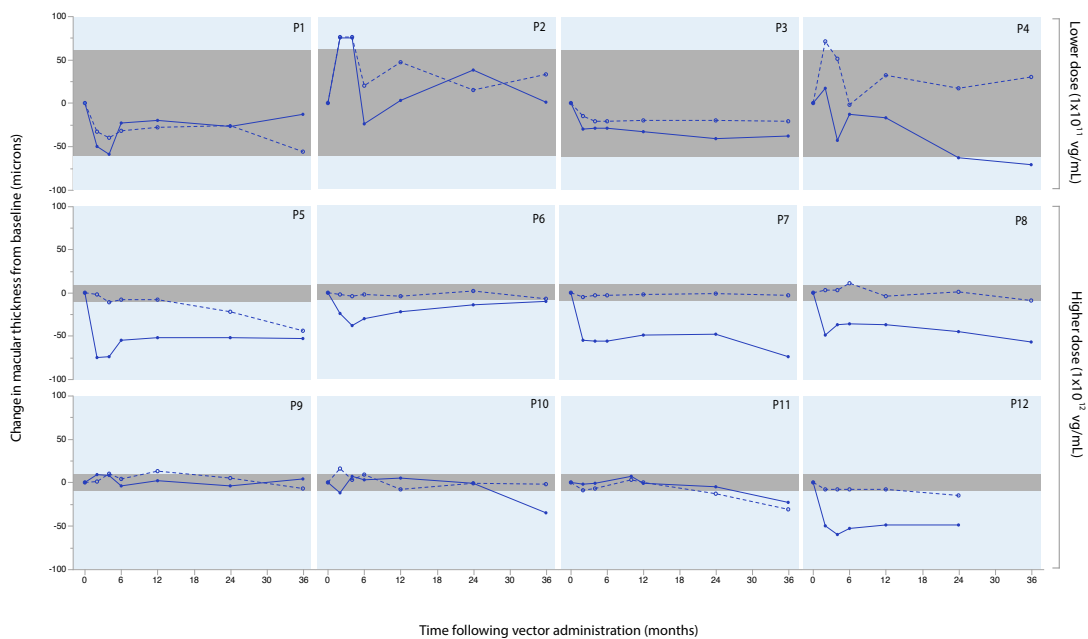
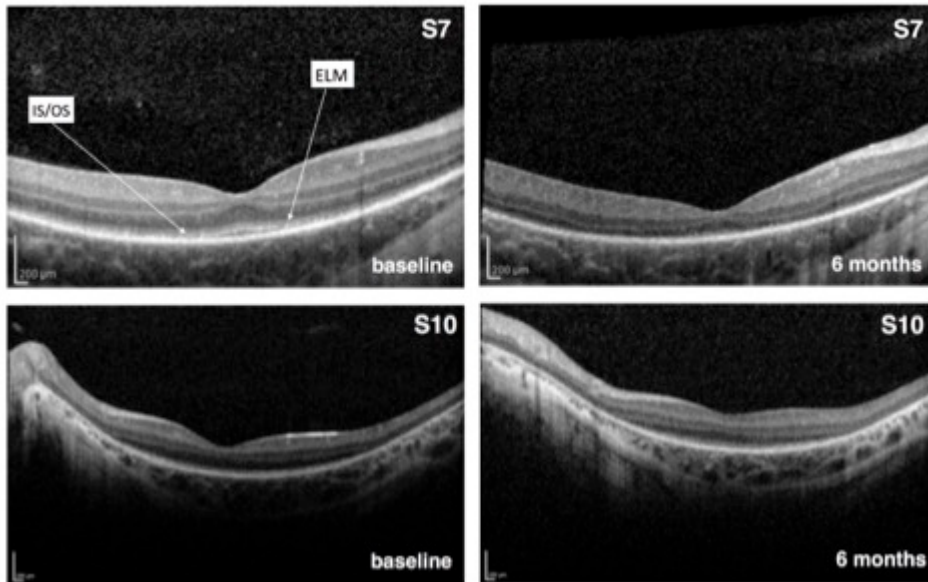


Fig S7b. Example OCT scans demonstrating disruption and thinning of the ellipsoid zone (IS/OS) and external limiting membrane (ELM) in Participant 7 (upper panels) after 6 months and, in contrast, preservation of intact ellipsoid zone in Participant 10 (lower panels). In both participants vector administration involved the fovea.



References

1. Bainbridge JW, Smith AJ, Barker SS, et al. Effect of gene therapy on visual function in Leber's congenital amaurosis. *N Engl J Med* 2008;358:2231-9.
2. Fitzke FW, Hitchings RA, Poinoosawmy D, McNaught AI, Crabb DP. Analysis of visual field progression in glaucoma. *The British journal of ophthalmology* 1996;80:40-8.
3. Weleber RG, Smith TB, Peters D, et al. VFMA: topographic analysis of sensitivity data from full-field static perimetry. *Translational Vision Science & Technology* 2015;In Press.
4. Bland JM, Altman DG. Measurement error. *Bmj* 1996;313:744.
5. Warriar KJ, Katz LJ, Myers JS, et al. A comparison of methods used to evaluate mobility performance in the visually impaired. *The British journal of ophthalmology* 2015;99:113-8.
6. Stockman A, Smithson HE, Michaelides M, Moore AT, Webster AR, Sharpe LT. Residual cone vision without alpha-transducin. *Journal of vision* 2007;7:8.
7. Pugh EN, Jr. Vision: Physics and Retinal Physiology. In: Atkinson RC, Herrnstein RJ, Lindsey G, Luce RD, eds. *Stevens' Handbook of Experimental Psychology, Second Edition*. New York: Wiley; 1988:75-163.
8. N. PE. Vision: Physics and Retinal Physiology. *Stevens' Handbook of Experimental Psychology*, R C Atkinson, R J Herrnstein, G Lindsey & R D Luce (Eds) 1998;1:75-163.
9. Leung CK, Cheung CY, Weinreb RN, et al. Comparison of macular thickness measurements between time domain and spectral domain optical coherence tomography. *Investigative ophthalmology & visual science* 2008;49:4893-7.
10. Annear MJ, Bartoe JT, Barker SE, et al. Gene therapy in the second eye of RPE65-deficient dogs improves retinal function. *Gene Ther* 2011;18:53-61.
11. Gearhart PM, Gearhart CC, Petersen-Jones SM. A novel method for objective vision testing in canine models of inherited retinal disease. *Invest Ophthalmol Vis Sci* 2008;49:3568-76.
12. Mowat FM, Breuwer AR, Bartoe JT, et al. RPE65 gene therapy slows cone loss in Rpe65-deficient dogs. *Gene Ther* 2013;20:545-55.
13. Bligh EG, Dyer WJ. A rapid method of total lipid extraction and purification. *Can J Biochem Physiol* 1959;37:911-7.
14. Chrispell JD, Feathers KL, Kane MA, et al. Rdh12 activity and effects on retinoid processing in the murine retina. *The Journal of biological chemistry* 2009;284:21468-77.